International Journal of Advances in Engineering and Management (IJAEM)
Volume 5, Issue 1 Jan. 2023, pp: 249-255 www.ijaem.net ISSN: 2395-5252

Exploring the Influence of Rotor Bar Taper Angle on Breakdown Torque using Machine Learning

Omogbai Nelson Oyakhilomen[1]; Anazia Emmanuel A.[2]; Anionovo Ugochukwu E[3].

[1,2,3]*Electrical Engineering Department, Nnamdi Azikiwe University, Awka, Anambra State, Nigeria.*
Corresponding Author: Omogbai, O.N.

Date of Submission: 01-01-2023 Date of Acceptance: 10-01-2023

ABSTRACT
The paper unveils the relative influence of the angle of taper of the squirrel cage induction motor rotor bar cross section, on the breakdown (maximum) torque of the machine. The influence of the top width and the radial depth of the bar section, as established design variables, were also investigated so as to know where the degree of influence of the taper angle falls in comparison, as far as the maximum torque is concerned. The machines were investigated in their steady state operating mode using the equivalent circuit method.The machine learning capabilities of the Least Square Support Vector Machine (LSSVM) was deployed to extract by prediction, information about the likely dependencies between the randomized block of the geometric variables and the breakdown torque,and the captured information was stored using the Root Mean Square Error (RMSE) of predictions. The validated results show that the rotor leakage reactance – a part determinant of the maximum torque; tends to be most sensitive to a design change in the taper angle of the transverse section of the rotor bar.

KEYWORDS: Taper angle, Breakdown torque, LSSVM, RMSE, rotor leakage reactance, Machine learning.

I. INTRODUCTION

The squirrel-cage induction motor (SCIM) happens to be the most adopted electrical machine for electrical drives [1]. Studies have shown that to improve the performance of a SCIM, several design variables may have to be modified; one of such adjustments being the optimization of the stator and rotor geometries [2].The rotor slot geometry which can be considered as an independent design parameter, is the most influential factor in defining the torque-speed characteristic of the SCIM, especially when mains fed [2],[3].

It was pointed out in [4] that between the small and large slip zones, mechanical characteristic exhibits a maximum, which corresponds to the highest torque obtained with given stator supply. A large breakdown torque is usually desirable either for high transient torque reserve or for widening the constant power speed range in variable frequency driven SCIMs [5]. A rotor slot shape that is deep and narrow, allows considerable magnetic flux to cross the slot. Large slot depth leads to a rather high rotor leakage inductance and thus a smaller breakdown torque. In [6], it was demonstrated that rectangular bar rotors produced more breakdown torque but less starting torque compared to the machine with stepped shape rotor.In their paper [2], the authors showed thata decrease of the bar reactance by implementing some design modifications like stepping of a portion of the transverse section, corresponds to the enhancement of the breakdown torque while the resistance played a minor role. It was also shown that at constant slot area, the optimization of the rated efficiency implies the maximization of both power factor and breakdown torque.The work of [7] in part, investigated the relative values of rotor leakage reactance for SCIM's with circular, oval, and rounded trapezoid rotor bar shapes. They discovered that the circular rotor bar has the least value of rotor leakage reactance and the largest flux linkage. Note that this circular geometry happens to be relatively the broadest (least taper) for the same rotor diameter and number of rotor slots. Also, the rounded trapezoid bar was found to have the largest rotor leakage reactance of the three shapes – it is clearly the most tapered of the investigated shapes.

In [8], it was highlighted also that a rotor current surge due to slip may raise the level of

International Journal of Advances in Engineering and Management (IJAEM)
Volume 5, Issue 1 Jan. 2023, pp: 249-255 www.ijaem.net ISSN: 2395-5252

leakage flux and thus, X_2. The author added that when the slot width increases, the overall slot permeance decreases as a result. This decreases the slot leakage flux and thus the leakage reactance of the stator or rotor.In [9], the authors emphasized that as the height of the rotor slot increases, permeance factor and slot inductance increases. Rotor leakage reactance is proportional to the leakage permeance. The torque developed is inversely proportional to rotor inductance [13]. By varying the slot width and height, the slot factor changes [9].The study in [10] made the observation that the average torque value decreased with increasing slot height value.Leakage flux is increased in narrow teeth because some of the flux is forced to seek alternate paths other than down the lengths of the teeth. Teeth that are too fat necessitate slots that are too narrow and result in slot leakage flux that is too high [11].

The researcher or designer in practice shall by the outcome of this study be able to ascertain critical variables of the bar section to focus on for the finetuning of the breakdown (T_{max}) torque, and together with other essential stator and rotor variables, may become more guided towards the optimal infeed to the computer algorithms/programs; for easier, more efficient and precise realization of distinct machine designs of target performance.

II. MATERIALS AND METHODS

First, two machines of 100 HP (M1) and 75HP (M2) were run in MATLAB for the purpose of conducting this study and their specifications are given in table 1

Second, all variables of machine M1 were kept constant while altering only the geometric parameters of the rotor bar cross section such as the top width (W), the radial depth (D), and the angle of taper (T); all varied at the same time. The maximum torque responses were recorded against the corresponding varied geometric parameters at each instance of variation, as far as the constraints were not violated and as far as the machine performance indices remain within acceptable limits.

Third, using the tunelssvm, trainlssvm and simlssvm commands from [14], the Least Square Support Vector Machine (LSSVM) was tuned and trained on one part of the collated data (namely, the training dataset) and deployed on the second part (namely, the various blocks of test dataset); to unravel by predicting with the randomized trial procedure, the levels of the underlying dependence that the breakdown torque may likely have on the various randomized blocks of the bar geometric parameters. The randomized blocks were investigated this way using the RMSE of the separate predictions as the metric of comparing the results. The following randomization was applied to the geometric parameter blocks of the rotor bar section:

Lone blocks – W (rotor bar top width), D (bar radial depth), and T (angle of taper).
Duo blocks – WT, DW. DT.
Triad blocks – WDT.
The most accurate results were then ranked in table 2.

All of the foregoing procedure were repeated with machine M2 which houses rotor bars of completely different design, so as to verify if the observed results are specific to a given machine design or generic within the family of the three-phase SCIMs. The block with the most accurate prediction (least RMSE) for each machine was noted and thoroughly analyzed with the relevant portions of literature, so as to properly situate, prune and finetune the Machine Learning(ML) result.

Table 1: Machine specification

Paramaters	M1	M2
Number of poles (p)	8	6
Number of rotor slots (Sr)	55	55
Number of stator slots (Ss)	72	72
Conductors per slot (Cs)	4	4
Full load efficiency (EffR) %	91.12268	91.01281
Full load current (I1R) Amps	137.6654	104.0402
Full load power factor (PFR)	0.858292	0.851315
Full load speed (nmR) rpm	738.5339	988.1062
Full load torque (TTdR) N.m	972.3505	545.2107
Starting Torque (Tst) N.m	1211.621	1033.852
Maximum Torque (Tmax) N.m	3368.963	2406.64
Starting Current (Ist) Amps	890.6528	875.9259
Bar current (Ib) Amps	604.1871	442.4421
End ring current (Ie) Amps	1322.191	1290.975
Voltage L-L (V) volts	400	400
X1 (ohms)	0.119191	0.109422
X2pr (ohms)	0.132793	0.136917
Xm (ohms)	3.939174	4.741772
R1 (ohms)	0.035604	0.055372
R2pr (ohms)	0.042764	0.049827
Rc (ohms)	110.508	157.5086

International Journal of Advances in Engineering and Management (IJAEM)
Volume 5, Issue 1 Jan. 2023, pp: 249-255 www.ijaem.net ISSN: 2395-5252

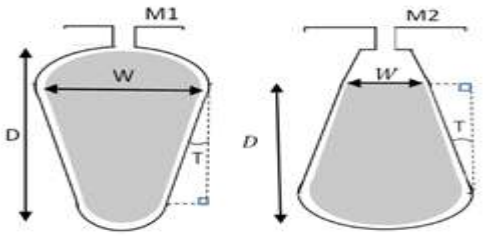

Fig 1: Rotor bar configurations

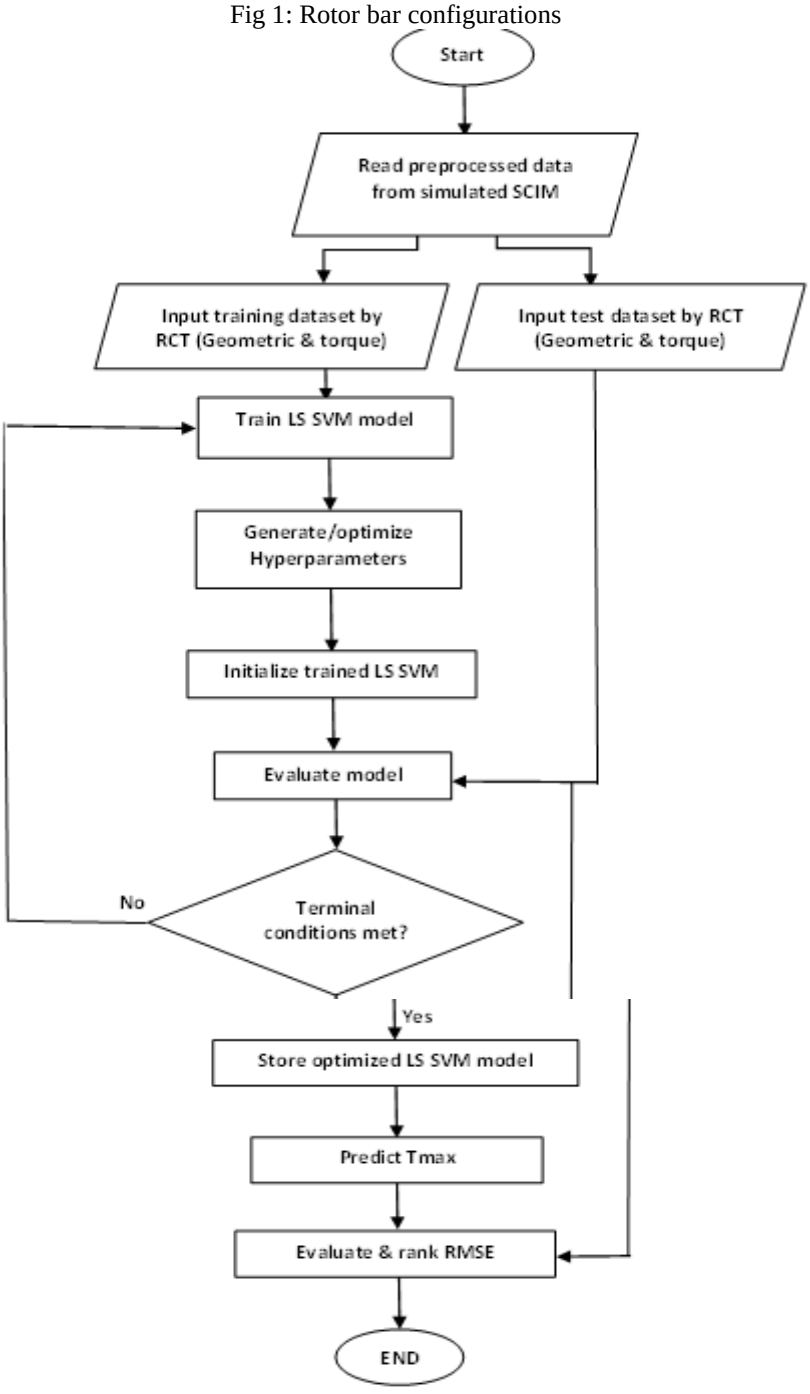

Fig 1,2: Machine learning flowchart

International Journal of Advances in Engineering and Management (IJAEM)
Volume 5, Issue 1 Jan. 2023, pp: 249-255 www.ijaem.net ISSN: 2395-5252

III. RESULTS AND DISCUSSION

Table 2: Results from machine learning

(M1) Geometric Blocks	(Tmax) RMSE		(M2) Geometric Blocks	(Tmax) RMSE
WT	5.12E-10		WT	8.69E-10
DT	5.26E-10		DT	1.24E-09
T	6.08E-10		T	1.28E-09

Table 2 shows that for both machines M1 and M2, the ML tends to put forward the geometric block WT as priority, as far as the influence of bar geometry on the breakdown or maximum torque is concerned. Also, among the investigated lone blocks of W, D and T; the T_{max} turns out to be most sensitive to design changes in the angle of taper – block T. According to [4];

$$T_{max} = \frac{3pU_{Srms}^2}{2L_{Ye}w_e^2} \quad (1.1)$$

In equation 1.1,U_S is the peak value of the phase voltages, p is the number of pole pairs, ω_e is the frequency of stator voltages, and currents, and inductance L_{Ye} represent the equivalent leakage inductance of the rotor and stator windings. For both of the investigated rotors, the simulated results in fig 2 show that the size of the angle of taper T seems to be directly proportional to the magnitude of the rotor leakage flux X_2 for reasons earlier discussed in the introduction. We understand from [11]that the leakage flux is increased in narrow teeth because some of the flux is forced to seek alternate paths other than down the lengths of the teeth. Also, a design increase in T, apart from encouraging a rise in X_2 through a rise in cross slot flux, will bring about a reduction in the cross-sectional area of the bar, and hence a consequent drop in the current at T_{max}. which will all culminate in a drop in T_{max}. Fig 3 depicts the X_2/T_{max} relationship from the simulated machines.

$T_{em} \alpha \phi . I_2 . (\text{rotor power factor})$ (1.2)

The work in [12] gives support to the X_2/Torque relation of fig 3 when he pointed out that a rise in X_2 connotes a drop in the rotor circuit power factor which means a decrease in torque production (T_{em}) according to expression 1.2, where ϕ and I_2 are respectively the airgap flux and rotor current.

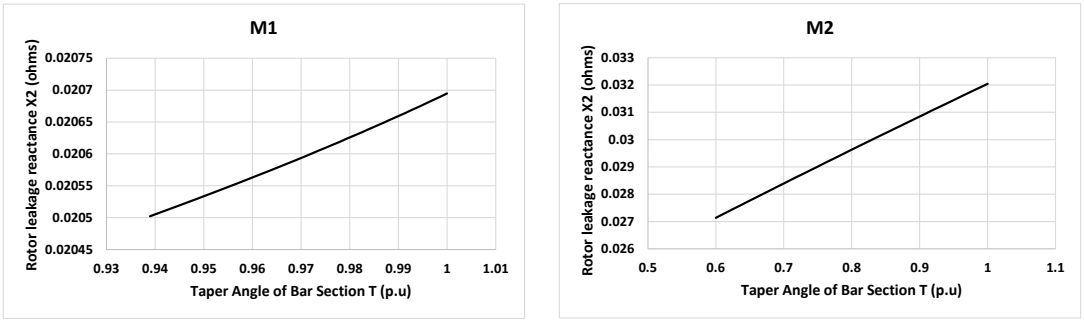

Fig 2: Influence of the angle of taper on the rotor leakage reactance

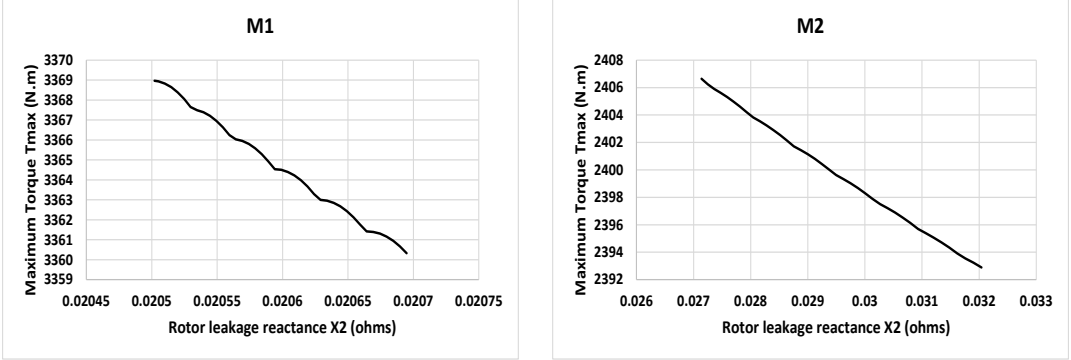

Fig 3: Influence of the rotor leakage reactance on the maximum torque.

International Journal of Advances in Engineering and Management (IJAEM)
Volume 5, Issue 1 Jan. 2023, pp: 249-255 www.ijaem.net ISSN: 2395-5252

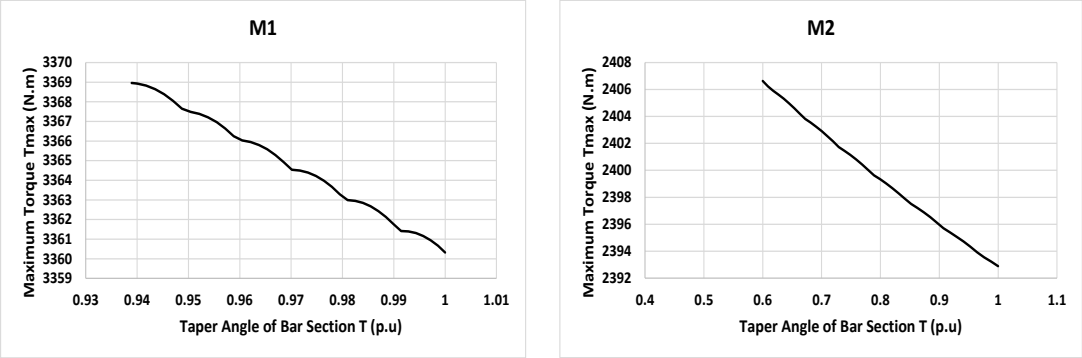

Fig 4: Influence of the angle of taper on the breakdown torque magnitude.

Also, fig 3 appears to corroborate equation 1.1 that there is an inverse relation between X_2 and T_{max}. These observations tend to align with literature. It may therefore be deduced from the foregoing discussions that there exists an inverse relation between the parameter T and T_{max} as fig 4 tends to depict from the responses of the simulated machines.

IV. TEST AND VALIDATION

It is to be tested that the cumulative influence of all variables of the rotor bar on the development of the maximum torque in particular, could also be largely achieved with the investigated variables – W and T only.To carry out this test, the experimental machine was again used and a reference case for two other variants of the same machine was chosen.The first variant – the base case was the case in which the dimensions of all the investigated parameters of the rotor bar were increased together from the reference case, so as to influence torque. The second variant was the control case, in which only the top width W and the angle of taper T were allowed to vary from the reference case as well. The W of both variants were the same, but the T was different since D was held constant for the control case.The bar radial depth D was kept constant by simply pegging it at the value for the reference case; since W and T can always vary without varying the radial depth.All cases were simulated and the results are given in table 3.

On comparing the base and control cases as in fig 5 and table 3, shows that when changes were made simultaneously to all the investigated geometric variables in the base case, a change of0.256% (3360 to 3369 Nm) from the reference values was observed in the T_{max}; while it was 3.25% (3260 to 3369 Nm) for the control case – a little difference of less than 3% exist between the base and control cases.The higher percentage for the control case could be attributed to the fact that the angle of taper was allowed to vary much more in the control case due to the fixed D. It may be observed from table 3 that the changes in X_2 tends to be dependent on the design changes in T more than it is on W or D. Therefore, because the control case has the largest angle of taper T, it tends to have the largest X_2 and therefore the lowest T_{max} as shown also in fig 5.

V. CONCLUSION

From the foregoing, it may be concluded that the exerted influence of the design modifications in T on X_2 and consequently on T_{max} seem to override the corresponding influence of W or D. In other words, among the investigated variables, X_2 or T_{max} appears to be most sensitive to the geometric changes in T.Therefore, within the accuracy bounds of the experimental methods and materials employed in this study, the designers, researchers and students working on the 3ph squirrel cage induction motor are herein presented with the taper angle of the rotor bar section, as a novel influential geometric variable with potentials that could arguably prove requisite for the infeed of torque optimization algorithms/programs.It therefore seems unnecessary to introduce avoidable complexity to the engineer's design algorithms/programs and eventually, a more error prone final solution; by inputting all availableT_{max} - influencing geometric parameters of the rotor, in the design and optimization routines, when just the angle of taper of the rotor bar as observed, could do the job remarkably well.

International Journal of Advances in Engineering and Management (IJAEM)
Volume 5, Issue 1 Jan. 2023, pp: 249-255 www.ijaem.net ISSN: 2395-5252

Table 3: Test results

	Maximum torque Tmax (N.m)	Rotor bar top Width W (mm)	Rotor bar radial depth D (mm)	Angle of bar taper T (Degrees)	X2 at Moderate slip (ohms)
Reference case	3368.962837	10.48168	25.15602	9.266795	0.0205021
Base case (W, D & T are varied)	3360.323546	11.60119	27.84286	9.869465	0.0206948
Control case (only W & T are varied)	3259.513839	11.60119	25.15602	12.8149	0.0207741

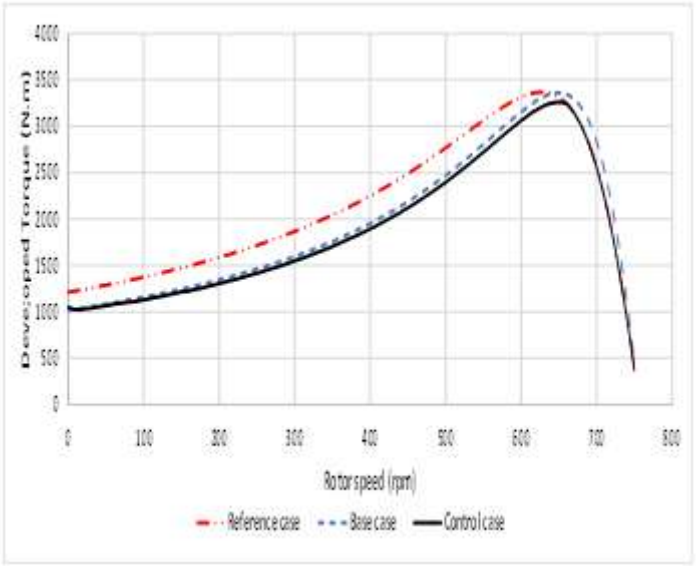

Fig 5: Test result

REFERNCES

[1]. Turcanu, O. A., Tudorache, T. and Fireteanu, T. (2006). Influence of squirrel-cage bar cross-section geometry on induction motor performances. A paper presented at the International Symposium on Power Electronics, Electrical Drives, Automation and Motion.in Sicily, Italy. held at Taormina on the 23 – 26 May, 2006.

[2]. Di Nardo, M., Marfoli, A., Degano, M., Gerada, C. and Chen, W. (2020). Rotor design optimization of squirrel cage induction motor - part II: results discussion. IEEE. 1 – 9. Doi: 10.1109/TEC.2020.3020263. 30 July, 2021.

[3]. Maloma, E., Muteba, M. and Nicolae, D., (2017). Effect of Rotor bar Shape on the Performance of Three Phase Induction Motors with Broken Rotor Bars. 2017 international conference on optimization of electrical an electronic equipment (OPTIM). 364 – 369. Doi:10.1109/OPTIM.2017.7974997. 17 September, 2021.

[4]. Vukosavic N. S. (2013). Electrical Machines. Springer New York Heidelberg Dordrecht London. ISBN: 978-1-4614-0400-2 (www.springer.com). DOI: 10.1007/978-1-4614-0400-2. Pp. 365 – 472.

[5]. Boldea, I. and Nasar, S. A. (2010). The Induction Machine Handbook. Washington, D.C: CRC Press, Taylor & Francis Group. PP. 447 – 473.

[6]. Fireteanu, V. (2008). Squirrel-Cage Induction Motor with Intercalated Rotor Slots of DifferentGeometries. XIII International Symposium on Electromagnetic Fields in Mechatronics, Electrical and Electronic Engineering, September, 2007. DOI: 10.3233/978-1-58603-895-3-284.

[7]. Purwanto, W., Sugiarto, T., Maksum, H., Martias, M., Nasir, M. and Baharudin, A. (2019). Optimal design of rotor slot geometry to reduce rotor leakage reactance and increase starting

performance for high-speed spindle motors. Advances in Electrical and Electronic Engineering. 17 (2). 96 – 105, Doi: 10.15598/aeee.v17i2.3170. 30 July, 2021.

[8]. Cochran, P. L. (1989). Polyphase Induction Motors. Analysis Design and Application. Marcel and Dekker. NY. USA. ISBN 0-8247-8043-4. Pp. 427 – 585.

[9]. Akhtar, M. J., Behera, R. K. and Parida, S. K. (2014). Optimized Rotor Slot Shape for Squirrel Cage Induction Motor in Electric Propulsion Application. IEEE 6th india international conference on power electronics (IICPE) 2014. 1 – 5. Dol: 0.1109/IICPE.2014.7115846. 17 September, 2021.

[10]. Yetgin, A. G. and Turan, M. (2016). Effects of rotor slot area on squirrel cage induction motor performance. International Journal of Innovative Science, Engineering & Technology. 3 (11),105 – 109. Retrieved from www.ijiset.com. on 29 July 2021.

[11]. Ho, S. (1996) Analysis and Design of AC Induction Motors With Squirrel Cage Rotors. Doctoral Dissertations. University of New Hampshire, Durham. Retrieved from: https://scholars.unh.edu/dissertation/1909, on 22 September, 2021.

[12]. Theraja, B. L., Theraja, A. K., (2008). A Textbook of Electrical Technology. S. Chand Publishing.

[13]. Gupta, J. B. (2013). Theory and Performance of Electrical Machines. S. K. Kataria and Sons. New Delhi, India. www.skkatariaandsons.com. Part III, Pp. 359 – 439.

[14]. De Brabanter, K., Karsmakers, P., Ojeda, F., Alzate, C., De Brabanter, J., Pelckmans, K., De Moor,B., Vandewalle, J., and Suykens, J.A.K. (2011). LS-SVMlab Toolbox User's Guide version 1.8. ESAT-SISTA Technical Report 10-146.http://www.esat